ADVANCED SUSTAINABLE SYSTEMS
www.advsustainsys.com

Inkjet-Printed Red-Emitting Flexible LEDs Based on Sustainable Inks of Layered Tin Iodide Perovskite

Giovanni Vescio, Dmitry N. Dirin, Sergio González-Torres, Jesús Sanchez-Diaz, Rosario Vidal, Iván P. Franco, Samrat Das Adhikari, Vladimir S. Chirvony, Juan P. Martínez-Pastor, Felipe A. Vinocour Pacheco, Lukasz Przypis, Senol Öz, Sergi Hernández, Albert Cirera, Iván Mora-Seró, Maksym V. Kovalenko, and Blas Garrido*

Inkjet printing has emerged as a promising technique for the fabrication of halide perovskite (HP) thin films, as it enables precise and controlled deposition of the perovskite ink on a variety of substrates. One main advantage of inkjet printing for the fabrication of HP thin films is its ability to produce uniform films with controlled thickness and high coverage, which is critical for achieving high-performance devices. Additionally, inkjet printing allows for the deposition of patterned thin films, enabling the fabrication of complex device architectures such as light-emitting diodes (LEDs). In this work, flexible LEDs based on inkjet printed Pb-free HP thiophene-ethylammonium tin iodide (TEA_2SnI_4) are produced that has gained attention as a potential alternative to Pb-based HPs in optoelectronic devices due to its lower toxicity, environmental impact, and high performance. The role of ink solutions is compared using pure solvents: toxic dimethyl formamide (DMF) and more eco-friendly dimethyl sulfoxide (DMSO). Red-emitting devices (λ_{max} = 633 nm) exhibit, in ambient conditions, a maximum external quantum efficiency (EQE_{max}) of 0.5% with a related brightness of 21 cd m^{-2} at 54 mA cm^{-2} for DMSO-based LEDs. The environmental impacts of films prepared with DMSO-based solvents ensure only 40% of the impact caused by DMF.

1. Introduction

Halide Perovskites (HPs) have attracted intensive attention over the past decade due to their excellent optoelectronic and semiconducting properties for an impressive variety of applications such as photovoltaics (PV) and perovskite-based light-emitting diodes (PeLEDs).[1] However, the toxicity and instability issues of the lead-based HPs severely restrict their practical applications for future commercialization and widespread adoption of HPs-based optical and electronic devices.[2–5] Lead is a cumulative toxicant that affects multiple body systems, including the neurological, hematological, gastrointestinal, cardiovascular, immune, and renal systems, with children being especially vulnerable to its neurotoxic effects.[6] Lead is included in the candidate list of substances of very high concern (SVHCs) for authorization for being toxic to reproduction. The authorization process, as outlined by the Regulations of the European Chemical Agency (REACH), aims to progressively replace

G. Vescio, S. González-Torres, S. Hernández, A. Cirera, B. Garrido
MIND-IN2UB
Department of Electronics and Biomedical Engineering
Universitat de Barcelona
Martí i Franquès 1, Barcelona 08028, Spain
E-mail: gvescio@ub.edu

The ORCID identification number(s) for the author(s) of this article can be found under https://doi.org/10.1002/adsu.202400060

DOI: 10.1002/adsu.202400060

D. N. Dirin, M. V. Kovalenko
Department of Chemistry and Applied Biosciences
ETH Zürich
Zürich CH-8093, Switzerland

D. N. Dirin, M. V. Kovalenko
Laboratory for Thin Films and Photovoltaics
Empa – Swiss Federal Laboratories for Materials Science and Technology
Dübendorf CH-8600, Switzerland

J. Sanchez-Diaz, I. P. Franco, S. D. Adhikari, I. Mora-Seró
Institute of Advanced Materials (INAM)
Universitat Jaume I (UJI)
Avenida de Vicent Sos Baynat, s/n, Castelló de la Plana 12071, Spain

R. Vidal, I. P. Franco
Department of Mechanical Engineering and Construction
GID
Universitat Jaume I
Av. SosBaynat s/n, Castelló 12071, Spain

SVHCs with less hazardous substances or technologies when technically and economically feasible alternatives are available. Lead content in electronics is restricted to mass concentrations lower than 0.1% in homogeneous materials through the "RoHS Directive".

Recently, there has been much work focused on Pb-free PeLEDs.[7–9] Among them the most promising family is 2D Sn-based devices [10,11] in virtue of the Sn^{2+} having the most similar to Pb^{2+} ionic radius and the similar electronic configuration (equivalent charge / charge neutrality/charge balance).[7,9] 2D tin halide perovskites offer an essential compromise between good optoelectronic properties but intrinsic instability of 3D Sn-based HPs and strongly localized Frenkel-like excitons in more stable 0D HPs.[12–15] Moreover, like the Pb-based counterparts the thin-films could be also prepared by facile synthesis based on solution-processed formation procedures, at room or relatively low temperature (< 180 °C). The substitution of Pb by Sn will allow us to comply with RoHS Directive European legislation and improve social health and perception. Lately, among the low-dimensional structures, 2D HPs present natural quantum well structures, large exciton binding energy, carrier confinement and higher thermal stability, photoluminescence (PL) narrow FWHM (full-width at half-maximum), and lifetime on the order of nanoseconds.[9,16]

Several studies have moved to improve the external quantum efficiency (EQE) of nanoscale 2D layered Sn 2D Sn-based HPs by fine-tuning the electronic properties of organic ammonium salts. Under optimized conditions, a PLQY of up to 21% was accomplished for the thienylethylammonium (TEA) Sn-iodide HPs (TEA_2SnI_4).[17] Another work demonstrates that ammonium thiocyanate (NH_4SCN) is an effective additive in enhancing the air stability of 2D TEA_2SnI_4, with emission decreasing less than 8% from its original value after exposure to air for 24 h, and photoluminescence quantum yield of 23%.[18] Among most of the studies on 2D Sn-based solutions in comparison with their Pb-containing PeLED counterpart, certainly, the most stable 2D nanoplates are considered the TEA_2SnI_4, whose emission is centered in the red region (≈634 nm)[9] and PEA_2SnI_4 from which we demonstrated inkjet-printed LEDs with red electroluminescence centered at ≈630 nm.[19–21]

V. S. Chirvony, J. P. Martínez-Pastor
UMDO
Instituto de Ciencia de los Materiales
Universidad de Valencia
Valencia 46980, Spain

F. A. Vinocour Pacheco
Saule Research Institute
Wroclaw 54-427, Poland

L. Przypis
Department of Semiconductor Materials Engineering
Wroclaw University of Science and Technology
Wroclaw 50-370, Poland

S. Öz
Saule Technologies
Wroclaw 54-427, Poland

S. Öz
Solaveni GmbH
59199 Bönen, Germany

Spin-coating has emerged as the predominant method for the fabrication of 2D Pb-free PeLED devices, consistently delivering commendable performance. Indeed, with this solution processable method, within the last year's most approaches and efforts have been dedicated to improving Sn-based LEDs focusing on inhibiting the oxidation of Sn^{2+}. This challenge has been addressed through various strategies, including the introduction of SnF_2 as a widely adopted additive, serving as a compensator for Sn^{2+}.[21] Additionally, novel approaches have been explored, such as the naphthol sulfonic salt is demonstrated as an effective multifunctional additive for LEDs with EQE of 0.72% and a brightness of 132 cd m^{-2},[22] or reducing agents such as $NaBH_4$,[21] or the aid of hypophosphorous acid (HPA) promoted PeLEDs with an EQE of 0.3% and a brightness of 70 cd m^{-2}.[23] Alternatively on one side is produced a PEA_2SnI_4 perovskite film with extremely low oxidation through a two-step recrystallization process with a resulting LED exhibiting a maximum EQE of 0.4%.[24]On the other side are prepared highly oriented 2D PEA_2SnI_4 nanoplates with low defect density obtaining devices with an EQE of 0.52% and 355 cd m^{-2}.[25]

Among all the works, the incorporation of valeric acid (VA), employed to reduce the Sn^{4+} content, facilitates PeLEDs with an EQE of 5%, at very low currents, and an operating half-life exceeding 15 h.[26] In the same way, very recently, LEDs based on TEA_2SnI_4 treated with cyanuric acid yielded an EQE of 20.29% and a half-lifetime of 27.6 h.[27] However, this high EQE is just obtained at very low currents and luminance around the turn-on voltage, decreasing one order of magnitude when significant luminance is demanded. Despite these results demonstrating the high potentiality of 2D Sn-based LEDs, all of them are affected by the use of toxic solvents involved in the perovskite fabrication process due to their compatibility with the commonly employed spin-coating technology.[28,29]

However, the investigation on Sn-based HP technologies is still in its infancy and further efforts are needed to use up-scalable deposition techniques to position these interesting materials up to the level of their Pb counterparts. Here we demonstrate the development of TEA_2SnI_4 LEDs with an industrially sustainable, low-cost deposition, and easy up scalable method/technology as inkjet printing.[30–33] In addition, the environmental impacts of the deposition are significantly reduced by the replacement of toxic solvents like N,N-dimethylformamide (DMF) with sustainable dimethyl sulfoxide (DMSO).[34–37] DMF is acknowledged as toxic to reproductive systems and is listed as SVHC under REACH. Conversely, DMSO is not classified as a hazard, although this does not mean that it does not cause environmental impacts. Therefore, the production and evaporation of DMSO, in comparison to DMF, result in lower environmental impacts and reduced human health toxicity.[27] In this regard, DMSO as a solvent was a critical factor in developing both lead and tin halide perovskites, owing to its ability to decrease the crystallization rate.

This stronger coordination of the DMSO with the formation of SnI_2·DMSO intermediate species facilitated more homogeneous nucleation and slower crystal growth.[29]

Inkjet printing does not allow for antagonist solvents, or antisolvents, so a solvent engineering process is needed to adjust the rheological properties of ink solutions and promote the stable/controlled formation of good uniformity crystalline perovskite phase. For this reason, we select neat DMSO, which is

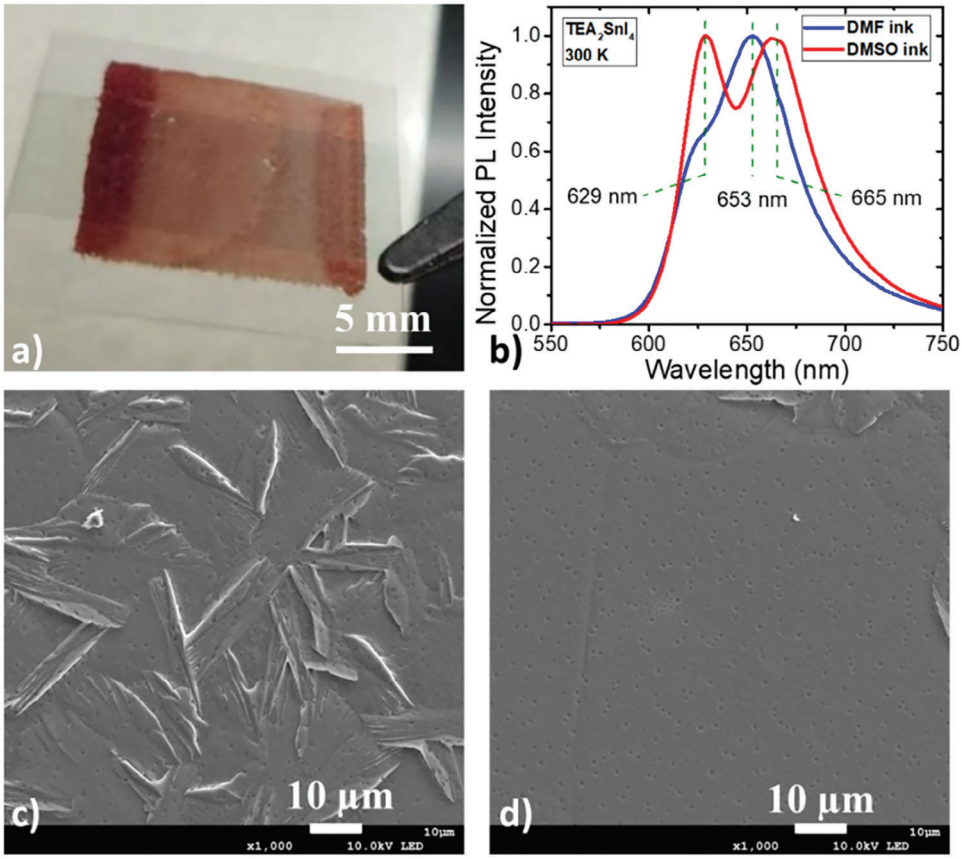

Figure 1. a) Inkjet-printed layer on PET substrate; b) room temperature normalized PL spectra of the films deposited by using DMF (red) and DMSO (blue) based inks; c,d) SEM top view images of inkjet-printed layer by using TEA_2SnI_4 ink DMF-based and DMSO-based solutions, respectively.

challenging due to its high boiling point (189 °C), in order to ensure stable ejection of a few picoliter droplets (10 pL) on the selected substrate and to guarantee the formation of higher quality crystallized films. This is due to the promotion of an inward Marangoni flow which acts in opposition to the preferential evaporation at the contact line that promotes an outward flow driving the 2D nanoplates to the edge.[32,38,39]

In this contribution, we analyze the role of two different ink solutions. The first one is based on the more common, but toxic, DMF solvent, and the second one is the green sustainable eco-friendly DMSO solvent. Both are used in the inkjet printing of TEA_2SnI_4 thin films to demonstrate that the eco-friendly TEA_2SnI_4 solvent should be taken into account in future advances for scalable optoelectronic Sn-based LEDs.

2. Device Structure and Fabrication

TEA_2SnI_4 thin films were deposited by inkjet-printed on a transparent flexible polyimide (PI) substrate (**Figure** 1a), without the use of antisolvent and any additive. Samples using common toxic DFM and green-friendly DMSO as solvent were prepared. Normalized photoluminescence (PL) spectra measured for both cases are shown in Figure 1b. As can be seen, both PL spectra consist of two bands, a short wavelength peaking at 629 nm for both types of inks and a long wavelength peaking at 653 nm for DMF-based inks and 665 nm for DMSO-based inks.

A very plausible scenario for this second broadband emission is the presence of dark excitonic states at ≈10 meV below the lowest radiative exciton[40] and defect-mediated (defect-induced) low-energy emission.[41] Several early studies show that the formation energy of Sn-related defects is low in Sn-based or mixed Sn—Pb HPs.[40–42] The dark states act as a reservoir for the excited population at ambient temperatures and thus enable, and do not necessarily hinder light emission is usually considered to be detrimental to luminescence efficiencies.[40]

For both films, strongly nonexponential PL decay kinetics are observed, well fitted by the sum of three exponentials, the average lifetime of which is 4.2 ns for the DMF-based ink and 2.4 ns for the DMSO-based ink, see Figure S1 (Supporting Information). The top-view scanning electron microscopy (SEM) images reveal that the inkjet-printed DMF layers without additives present nonuniform films with abundant wrinkles due to large grain boundaries, see Figure 1c. On the other hand, thin films with DMSO are more homogeneous, and they exhibit a larger scale uniformity, see Figure 1d. Consequently, samples prepared with DMSO present enhanced morphology in comparison with DMF-prepared samples.

Moreover, we observed that the rheological properties of the ink solutions play an important role during drop ejection and contact pinning with the substrate. Indeed, many factors are simultaneously acting in the case of inkjet printing technology. Mainly the very small droplet volumes, from 2.4 to 10 pL, and

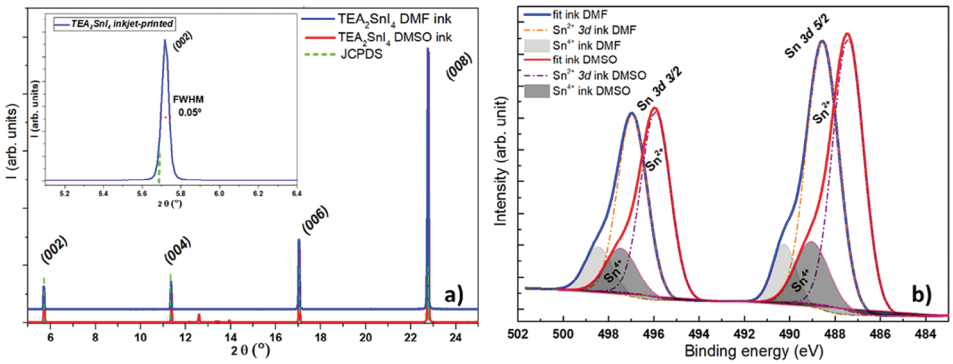

Figure 2. a) XRD pattern of inkjet-printed TEA_2SnI_4 after vacuum annealing showing the main preferential crystallographic planes according to tetragonal phase in literature;[42] detail of high-resolution XRD spectra (in the range from 5° to 6.5°) of TEA_2SnI_4 films (inset); b) XPS binding energy survey high-resolution XPS spectra of Sn 3d 3/2 and 3d 5/2 in annealed inkjet-printed thin film.

their fast evaporation during the flight reaching the substrate promote at that moment a specific ratio solvent/solute at the surface which allows for a better or worse perovskite crystallization. Aware of the boiling point of the ink solution, homogeneous and uniform pinholes free thin films could be achieved by controlling the droplet speeds, distance from the substrate, platen temperature, and post processing annealing step.

The quality of inkjet printed layers in DMF and DMSO submitted to different postannealing temperatures has been determined by X-ray diffraction. Then, we found that the best temperature of post annealing process was 85 °C (DMF) and 110 °C (DMSO) by an in-depth study of XRD versus thermal curing temperature. The diffraction patterns, acquired from the printed TEA_2SnI_4 thin films, display clearly the same characteristic reflections *(00l)* for both proposed samples, see **Figure** 2a. This characteristic 2D crystallization phase is strictly correlated to the complete evaporation of solvents. From the enlarged XRD patterns, we observe that the (002) diffraction peak is located at 5.7°, as expected from the d-spacing values of TEA_2SnI_4 planes, 15.5 Å.[43]

X-ray photoelectron spectroscopy (XPS) analysis was performed to investigate the chemical environment and composition of inkjet-printed _HP films. We monitored and assessed the oxidation of Sn^{2+} to Sn^{4+}, which affects the stability of Sn-HP thin films based on DMF and DMSO solvents. As shown in Figure S2 (Supporting Information) the wide energy survey spectrum exhibited the distinctive peaks of TEA_2SnI_4 bonds, with their corresponding binding energies (BE).[43] An analysis of these peaks revealed that 488.5 and 496.9 eV correspond to the $3d_{5/2}$ and $3d_{3/2}$ doublet of the Sn 3d spin-orbit doublet characteristic of TEA_2SnI_4.[18,27,42]

We obtained high-resolution (HR) XPS spectra of Sn to reveal the formation of Sn^{4+}, which is present in a small amount. The HR-XPS spectra, see Figure 2b, of the inkjet-printed TEA_2SnI_4 thin films show that the oxidation of the Sn-HP is almost completely moderate with a component less than 8% for DMF and 10% for DMSO inkjet-printed layers, respectively. These ratios of Sn^{4+}/Sn^{2+} from the XPS spectra are comparable to the best obtained in the literature.[27,43]

Thus, all the results indicate that the TEA_2SnI_4 in DMSO inkjet-printed thin films show good uniformity, absence of roughness, high degree of crystallinity with large domains, low oxidation of Sn^{+2}, and improved light emission in comparison to solutions with DMF, which make them a promising nontoxic metal halide perovskite material for fabrication of red-emitting LEDs for wearable photonics technology.

We have estimated the TEA_2SnI_4 band gap to be ≈1,85 eV (red) from the absorption measurements, by arranging the data into the Tauc plot after subtracting the excitonic emission seen at room temperature; this excitonic emission is indeed an indication of the high quality of the samples, see Figure S3 (Supporting Information). Taking into account the conduction and the valence band offsets, for accurate electron and hole injection we selected PEDOT:PSS (poly(3,4-ethylenedioxythiophene:polystyrenesulfonate) and POT2T (2,4,6-tris[3(diphenylphosphinyl)phenyl]−1,3,5-triazine) as hole and electron transport layers as shown by the energy level diagram and the configuration of the devices in **Figure** 3a. We manufactured the Sn-based PeLEDs with the following process: TEA_2SnI_4 thin films (≈100 nm) were inkjet-printed onto PEDOT:PSS-coated (30 nm) prepatterned ITO (100 nm) on glass substrates from a DMF or a DMSO solution containing TEAI and SnI_2 (0.25 molar ratio) followed by vacuum annealing at 100 °C (15′). Then, the device architecture is completed by the evaporated POT2T (40 nm)/ LiF (1 nm) / Al (170 nm),[44] as illustrated in Figure 3b by a sketch diagram and a corresponding real device under bending stress, see Figure 3c. Following the device characterization experiments were performed under ambient conditions after a proper encapsulation, see Figure 3d.

3. Results

As far as we know this work reports the first inkjet-printed TEA_2SnI_4 LED. The electroluminescence (EL) spectral characteristics with both solvents, are pure red with a peak centered at 633 nm with FWHM of 29 nm as a function of the applied voltages, see **Figure** 4a. Figure 4b,c presents the current density and luminance as a function of the operating voltage of inkjet-printed devices using both proposed solvents (16-emitting components). Using the eco-friendly DMSO solvent is clearly ensuring comparable performances of DMF solvent-based LEDs. For DMF the threshold turn-on voltage is ≈2.25 V and for the DMSO is lower ≈1.75 V. Moreover, it can be seen that the current density of the DMF devices reaches 20 mA cm^{-2} and drops after an applied voltage of 3.75 V. This is probably caused mainly by the

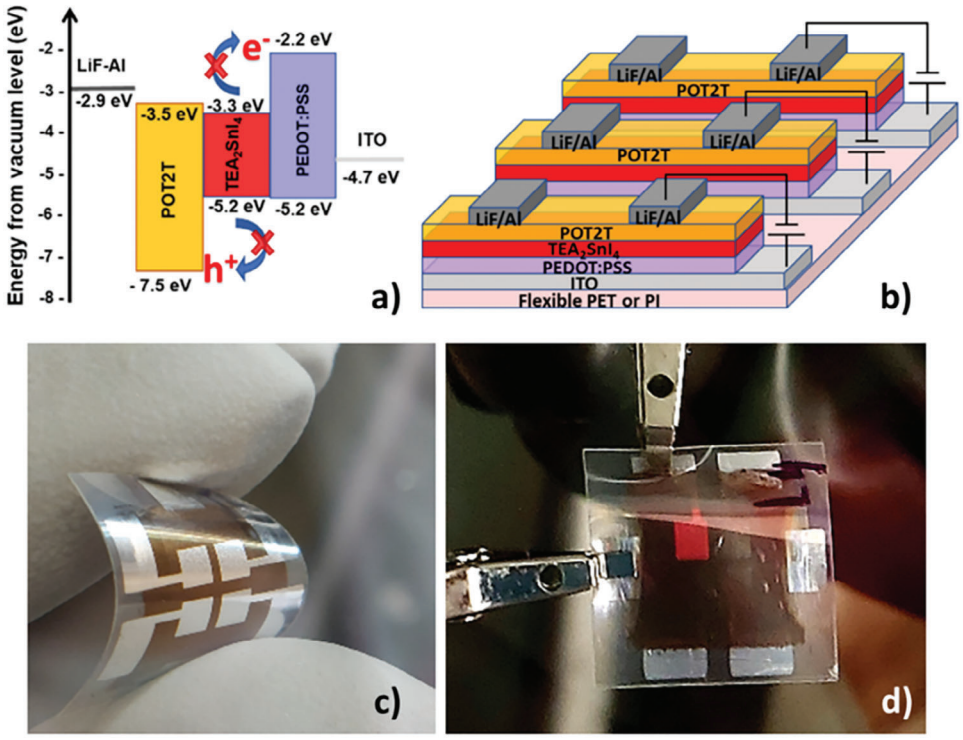

Figure 3. a) Energy band diagram for the proposed architecture; b) 3D sketch of the multi-pixels inkjet-printed TEA_2SnI_4 LEDs. c,d) Images of complete LED devices under bending stress and emitting pixel into the glovebox operating at 3.5 V.

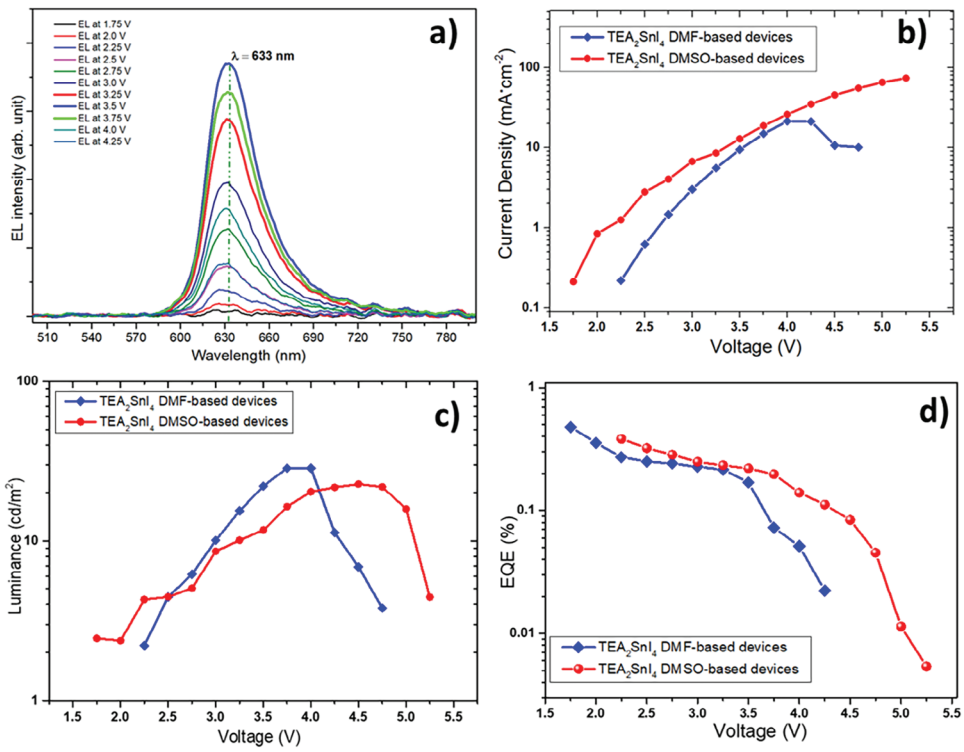

Figure 4. a) EL spectral characteristics of inkjet-printed TEA_2SnI_4 devices is red emitting with a peak centered at 633 nm with FWHM of 29 nm at different operation voltages. b,c) Current density and luminance versus voltage characteristics on a flexible substrate. The results for LEDs with inkjet printed TEA_2SnI_4 film prepared with DMF-based and DMSO-based solvents. d) EQE versus voltage characteristics.

thermal–electrical stress the device is subjected at interfaces during emission. On the other hand, DMSO-based devices are more stable up to 5.25 V and attain 75 mA cm^{-2}. Nevertheless, the luminance data of both configurations are comparable. Indeed, the device using DMF as a solvent reaches values of luminance being the maximum 28 cd m^{-2} whereas DMSO has its ≈21 cd m^{-2}. Just slightly higher values have been obtained on the glass substrate as presented in Figure S4 (Supporting Information).

The electrical behavior analysis of the luminance versus the correlated current densities curves characteristics of both devices presents two possible different mechanisms of emission. The linear tendency with a slope ≈1.08 of DMSO curve characteristic (Figure S5, Supporting Information) can be associated with the general expected spontaneous emission; likewise, the DMF-based devices show also a linear trend but with a higher slope of 1.85, which might be due to additional recombination due to less uniform material and the p-type character of the perovskite (due to Sn^{+4} formation).[15] Correspondingly, the EQE, plotted as a function of voltage, verifies the tendency, see Figure 4d, for all samples employing both DMF or DMSO solvents, respectively. The peak EQE of the devices with each solvent is ≈0.5%. This value is very promising and not far from the most efficient reported red lead-free LED by spin-coating method.[23,27,45]

Although not the highest reported brightness for Pb-free perovskite LED, close to 30 cd m^{-2}, considering the state-of-the-art we reported the lowest voltage threshold, the second highest EQE (the highest at high current), and the 3rd highest luminance.

We present an example of working devices and the possibility of controlling each pixel one by one as shown in Video S1 (Supporting Information). The carried out CIE coordinates are (0.695, 0.305,) close to the ideal red color coordinate for Rec. 2100 specifications for a primary red emitter (0.708, 0.292) as shown by Figure S6 (Supporting Information).

4. Environmental Concerns

Up-scaling development of HP LEDs will require not just the use of appropriate deposition techniques, such as inkjet printing, but also low-impact materials. This inkjet-printed TEA_2SnI_4 LED avoids the use of lead and DMF as solvents. In addition to the toxicity concerns, DMF adversely affects the maintenance of cartridges and printheads. However, the higher boiling temperature and increased viscosity of DMSO contribute to higher electricity consumption during perovskite deposition.

To ascertain the perovskite ink with the lowest environmental impact, a comparative life cycle assessment (LCA) was conducted in accordance with ISO standards (14 040/14 044). LCA is a methodology for evaluating the environmental burdens associated with a product or process by identifying and quantifying energy and materials used, as well as the wastes released to the environment. It assesses the impact of these energy and material uses and releases and identifies opportunities for environmental improvements. The comparative functional unit was one square centimeter of perovskite ink printed. The LCA inventory includes only the differences between the printing inks with DMF and DMSO as solvents. The composition and quantity of the perovskite are the same for both inks and are therefore not included in this LCA. Differences in the experimental procedure for perovskite layer deposition with DMF and DMSO are explained in the section "Inkjet printing and thermal treatments of TEA_2SnI_4 layer" of the Supporting Information. The differences between the inks pertain to the quantity and type of solvent needed for the solution of perovskite, electricity consumption during printing and annealing, air emissions of solvents during drying, and the differential wear of cartridges and printheads, categorized into manufacturing and end-of-life (EOL). Life cycle inventories and evaluation impacts are presented in the Supporting Information.

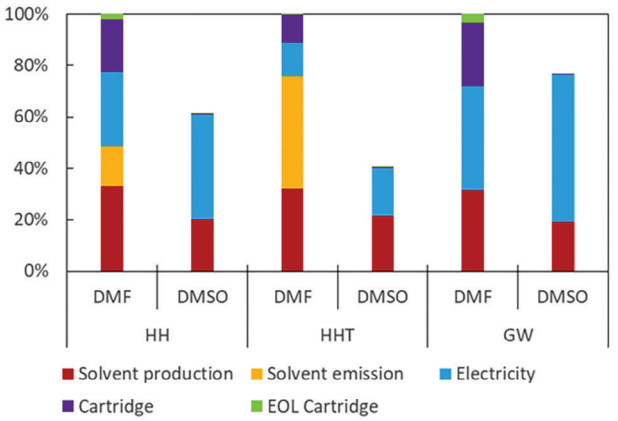

Figure 5. Comparative environmental assessment of inkjet printed TEA_2SnI_4 film prepared with DMF-based and DMSO-based solvents. HH: Total human health impact category, including human health toxicity (HHT) and global warming (GW).

For the purpose of comparison, **Figure 5** focuses on the human health area of protection (HH) and the two primary impact categories within it: human health toxicity (HHT) and global warming (GW). The impacts of DMSO are significantly lower, at 61%, 40%, and 77% in the categories of HH, HHT, and GW, respectively, when compared to those of DMF. The human health toxicity associated with DMSO is negligible in contrast to DMF, as discernible in the HH and HHT impact categories. It is essential to highlight the impact across all categories due to the increased utilization of cartridges and printheads with DMF perovskite inks. Additionally, DMF production results in higher impacts compared to DMSO manufacturing. Nevertheless, the elevated electricity consumption during the printing and annealing of perovskite ink with DMSO is evident in the GW and HH impact categories. These impacts are particularly sensitive to the energy mix and would be exacerbated in countries with a higher percentage of fossil resources.

Our analysis was focused only on showing the differences between printed tin halide perovskite films prepared with two different solvents. Future life cycle assessments should address the entire LED device, which will allow comparisons with lead perovskite LEDs. At this time, the efficiency and durability of the Sn-based LEDs is still very low and thus the cradle-to-grave LCA is too uncertain to proceed with comparisons to other LEDs. The need for a vacuum required for the manufacture of Sn-based LEDs, which means higher energy consumption and nitrogen emissions, not to mention the problems of industrial scale-up, is certainly a drawback compared to the manufacture of lead-based LEDs.

5. Conclusion

We have successfully shown the pure red-emitting LEDs based on TEA_2SnI_4 2D perovskites inkjet-printed on flexible substrates, demonstrating the potential and scalability of this technology. We have overcome the degradation and instability issues of Sn-based solutions by using DMSO as a more sustainable and eco-friendly solvent than the commonly used toxic DMF. DMSO-based inks have optimal rheological properties for inkjet printing technology and promote fast crystallization during vacuum annealing. The inkjet-printed TEA_2SnI_4-based LED shows a maximum external quantum efficiency (EQE) of 0.5% and a brightness of 28 (DMF) and 21 cd m^{-2} (DMSO) in ambient conditions after encapsulation. These values are comparable to those of the spin-coated control devices and are the first reported for inkjet-printed TEA_2SnI_4-based LEDs. The impacts of films prepared using DMSO-based solvents are notably diminished, with reductions of 61%, 40%, and 77% observed in the categories of human health, human health toxicity, and global warming, respectively, when contrasted with those associated with DMF. Certainly, future priorities will involve further optimization through the incorporation of appropriate additives compatible with DMSO and inkjet printing. It is noteworthy to mention that the achieved values, obtained when using near-pristine precursor solutions, align with or surpass most comparable achievements documented in the literature.

Supporting Information

Supporting Information is available from the Wiley Online Library or from the author.

Acknowledgements

The authors wish to thank the financial support from the European Commission via FET Open Grant (862656, DROP-IT), This work has been partially funded by Ministry of Science and Innovation of Spain under project LIP-FREE (PID2022-140978OB-I00), under project PIXIE-SENS (PDC2023-145804-I00), and under project PLEDs (PID2022-140090OB-C21) and by Generalitat Valenciana under Print-P (MFA/2022/020) project.

Conflict of Interest

The authors declare no conflict of interest.

Data Availability Statement

The data that support the findings of this study are available from the corresponding author upon reasonable request.

Keywords

flexible technology, green solvent, inkjet printing, lead-free perovskite, LED

Received: January 22, 2024
Revised: March 24, 2024
Published online:

[1] Z. Xiao, R. A. Kerner, L. Zhao, N. L. Tran, K. M. Lee, T. W. Koh, G. D. Scholes, B. P. Rand, *Nat. Photonics* **2017**, *11*, 108.
[2] C. Pareja-Rivera, D. Morett, D. Barreiro-Argüelles, P. Olalde-Velasco, D. Solis-Ibarra, *J. Physics: Energy* **2021**, *3*, 032014.
[3] R. Wang, J. Wang, S. Tan, Y. Duan, Z. K. Wang, Y. Yang, *Trends Chem* **2019**, *1*, 368.
[4] J. Li, J. Duan, X. Yang, Y. Duan, P. Yang, Q. Tang, *Nano Energy* **2021**, *80*, 105526.
[5] F. Zhang, Z. Ma, Z. Shi, X. Chen, D. Wu, X. Li, C. Shan, *Energy Material Advances* **2021**, *2021*, 1.
[6] World Health Organization. Preventing Disease through Healthy Environments: Exposure to Lead: A Major Public Health Concern **2019**.
[7] E. V. Ushakova, S. A. Cherevkov, V. A. Kuznetsova, A. V. Baranov, *Materials* **2019**, *12*, 3845.
[8] T. Xuan, R.-J. Xie, *Chem. Eng. J.* **2020**, *393*, 124757.
[9] X. Li, X. Gao, X. Zhang, X. Shen, M. Lu, J. Wu, Z. Shi, V. L. Colvin, J. Hu, X. Bai, W. W. Yu, Y. Zhang, *Adv. Sci.* **2021**, *8*, 2003334.
[10] X. Zhang, C. Wang, Y. Zhang, X. Zhang, S. Wang, M. Lu, H. Cui, S. V. Kershaw, W. W. Yu, A. L. Rogach, *ACS Energy Lett.* **2019**, *4*, 242.
[11] Y. Gao, Y. Pan, F. Zhou, G. Niu, C. Yan, *J Mater Chem A Mater* **2021**, *9*, 11931.
[12] C. C. Stoumpos, D. H. Cao, D. J. Clark, J. Young, J. M. Rondinelli, J. I. Jang, J. T. Hupp, M. G. Kanatzidis, *Chem. Mater.* **2016**, *28*, 2852.
[13] D. N. Dirin, A. Vivani, M. Zacharias, T. V. Sekh, I. Cherniukh, S. Yakunin, F. Bertolotti, M. Aebli, R. D. Schaller, A. Wieczorek, S. Siol, C. Cancellieri, L. P. H. Jeurgens, N. Masciocchi, A. Guagliardi, L. Pedesseau, J. Even, M. V. Kovalenko, M. I. Bodnarchuk, *Nano Lett.* **2023**, *23*, 1914.
[14] L. Mao, C. C. Stoumpos, M. G. Kanatzidis, *J. Am. Chem. Soc.* **2019**, *141*, 1171.
[15] L. Zhang, C. Sun, T. He, Y. Jiang, J. Wei, Y. Huang, M. Yuan, *Light Sci Appl* **2021**, *10*, 61.
[16] J. Lu, C. Yan, W. Feng, X. Guan, K. Lin, Z. Wei, *EcoMat* **2021**, *3*, 1.
[17] J. T. Lin, C. C. Liao, C. S. Hsu, D. G. Chen, H. M. Chen, M. K. Tsai, P. T. Chou, C. W. Chiu, *J. Am. Chem. Soc.* **2019**, *141*, 10324.
[18] J. T. Lin, Y. K. Hu, C. H. Hou, C. C. Liao, W. T. Chuang, C. W. Chiu, M. K. Tsai, J. J. Shyue, P. T. Chou, *Small* **2020**, *16*, 2000903.
[19] J. Zhang, X. Zhu, M. Wang, B. Hu, *Nat. Commun.* **2020**, *11*, 1.
[20] L. Lanzetta, J. M. Marin-Beloqui, I. Sanchez-Molina, D. Ding, S. A. Haque, *ACS Energy Lett.* **2017**, *2*, 1662.
[21] G. Vescio, J. Sanchez-Diaz, J. L. Frieiro, R. S. Sánchez, S. Hernández, A. Cirera, I. Mora-Seró, B. Garrido, *ACS Energy Lett.* **2022**, *10*, 3653.
[22] Y. J. Heo, H. J. Jang, J. H. Lee, S. B. Jo, S. Kim, D. H. Ho, S. J. Kwon, K. Kim, I. Jeon, J. M. Myoung, J. Y. Lee, J. W. Lee, J. H. Cho, *Adv. Funct. Mater.* **2021**, *31*, 2106974.
[23] F. Yuan, X. Zheng, A. Johnston, Y. Wang, C. Zhou, Y. Dong, B. Chen, H. Chen, J. Z. Fan, G. Sharma, P. Li, Y. Gao, O. Voznyy, H. Kung, Z. Lu, O. M. Bakr, E. H. Sargent, *Sci Adv.* **2020**, *6*, eabb0253.
[24] Y. H. Cheng, R. Moriyama, H. Ebe, K. Mizuguchi, R. Yamakado, S. Nishitsuji, T. Chiba, J. Kido, *ACS Appl. Mater. Interfaces* **2022**, *14*, 22941.
[25] Y. Liao, Y. Shang, Q. Wei, H. Wang, Z. Ning, *J Phys D Appl Phys* **2020**, *53*, 414005.
[26] H. Liang, F. Yuan, A. Johnston, C. Gao, H. Choubisa, Y. Gao, Y. K. Wang, L. K. Sagar, B. Sun, P. Li, G. Bappi, B. Chen, J. Li, Y. Wang, Y. Dong, D. Ma, Y. Gao, Y. Liu, M. Yuan, M. I. Saidaminov, S. Hoogland, Z. H. Lu, E. H. Sargent, *Adv. Sci.* **2020**, *7*, 1903213.
[27] D. Han, J. Wang, L. Agosta, Z. Zang, B. Zhao, L. Kong, H. Lu, I. Mosquera-Lois, V. Carnevali, J. Dong, J. Zhou, H. Ji, L. Pfeifer, S. M. Zakeeruddin, Y. Yang, B. Wu, U. Rothlisberger, X. Yang, M. Grätzel, N. Wang, *Nature* **2023**, *622*, 493.

[28] R. Vidal, J. A. Alberola-Borràs, S. N. Habisreutinger, J. L. Gimeno-Molina, D. T. Moore, T. H. Schloemer, I. Mora-Seró, J. J. Berry, J. M. Luther, *Nat. Sustain.* **2021**, *4*, 277.
[29] J. Pascual, D. Di Girolamo, M. A. Flatken, M. H. Aldamasy, G. Li, M. Li, A. Abate, *Chem. – A Eur. J.* **2022**, *28*, 202103919.
[30] G. Vescio, J. López-Vidrier, R. Leghrib, A. Cornet, A. Cirera, *J Mater Chem C Mater* **2016**, *4*, 1804.
[31] K. Zhu, G. Vescio, S. González-Torres, J. López-Vidrier, J. L. Frieiro, S. Pazos, X. Jing, X. Gao, S. D. Wang, J. Ascorbe-Muruzábal, J. A. Ruiz-Fuentes, A. Cirera, B. Garrido, M. Lanza, *Nanoscale* **2023**, *15*, 9985.
[32] G. Vescio, J. L. Frieiro, A. F. Gualdrón-Reyes, S. Hernández, I. Mora-Seró, B. Garrido, A. Cirera, *Adv. Mater. Technol.* **2022**, *7*, 2101525.
[33] S. González, G. Vescio, J. L. Frieiro, A. Hauser, F. Linardi, J. López-Vidrier, M. Oszajca, S. Hernández, A. Cirera, B. Garrido, *Adv. Mater. Interfaces* **2023**, *10*, 2300035.
[34] Y. Wang, F. Zhang, J. Ma, Z. Ma, X. Chen, D. Wu, X. Li, Z. Shi, C. Shan, *EcoMat* **2022**, *4*, 1.
[35] V. Stancu, A. G. Tomulescu, L. N. Leonat, L. M. Balescu, A. C. Galca, V. Toma, C. Besleaga, S. Derbali, I. Pintilie, *Coatings* **2023**, *13*, 378.
[36] E. Radicchi, E. Mosconi, F. Elisei, F. Nunzi, F. De Angelis, *ACS Appl. Energy Mater.* **2019**, *2*, 3400.
[37] S. K. Podapangi, F. Jafarzadeh, S. Mattiello, T. B. Korukonda, A. Singh, L. Beverina, T. M. Brown, *RSC Adv.* **2023**, *13*, 18165.
[38] D. Soltman, V. Subramanian, *Langmuir* **2008**, *24*, 2224.
[39] G. Vescio, G. Mathiazhagan, S. González-Torres, J. Sanchez-Diaz, A. Villaueva-Antolí, R. S. Sánchez, A. F. Gualdrón–Reyes, M. Oszajca, F. Linardi, A. Hauser, F. A. Vinocour-Pacheco, W. Żuraw, S. Öz, S. Hernández, I. Mora-Seró, A. Cirera, B. Garrido, *Adv. Eng. Mater.* **2023**, *2300927*, 1.
[40] G. Folpini, D. Cortecchia, A. Petrozza, A. R. Srimath Kandada, *J Mater Chem C Mater* **2020**, *8*, 10889.
[41] H. H. Fang, E. K. Tekelenburg, H. Xue, S. Kahmann, L. Chen, S. Adjokatse, G. Brocks, S. Tao, M. A. Loi, *Adv. Opt. Mater.* **2023**, *11*, 202202038.
[42] H. H. Fang, S. Adjokatse, S. Shao, J. Even, M. A. Loi, *Nat. Commun.* **2018**, *9*, 243.
[43] Z. Wang, F. Wang, B. Zhao, S. Qu, T. Hayat, A. Alsaedi, L. Sui, K. Yuan, J. Zhang, Z. Wei, Z. Tan, *J. Phys. Chem. Lett.* **2020**, *11*, 1120.
[44] K. M. M. Salim, E. Hassanabadi, S. Masi, A. F. Gualdrón-Reyes, M. Franckevicius, A. Devižis, V. Gulbinas, A. Fakharuddin, I. Mora-Seró, *ACS Appl Electron Mater* **2020**, *2*, 2525.
[45] H. Liang, F. Yuan, A. Johnston, C. Gao, H. Choubisa, Y. Gao, Y. K. Wang, L. K. Sagar, B. Sun, P. Li, G. Bappi, B. Chen, J. Li, Y. Wang, Y. Dong, D. Ma, Y. Gao, Y. Liu, M. Yuan, M. I. Saidaminov, S. Hoogland, Z. H. Lu, E. H. Sargent, *Adv. Sci.* **2020**, *7*, 1903213.